Determination of the Critical Velocity of Molten Metal Flow in Casting Mould Sprue

Francis Inegbedion[*1], John A. Akpobi[2]

[*1]Department of Production Engineering, University of Benin, Benin City, Nigeria
[2]Department of Production Engineering, University of Benin, Benin City, Nigeria

Abstract *- Casting is a manufacturing process in which molten metal is poured through a gating system to fill a mould cavity where it solidifies. Variations in casting parameters chosen by different researchers have led to significant variations in casting guidelines. These have forced foundry-men to carry out a number of trial and error runs to create guidelines based on their own experience. This has resulted in defects occurring in casting during the mould filling process. The authors aimed at determining the critical height and critical velocity of molten metal flow in the mould sprue. The continuity equation was used to describe the velocity distribution of the molten metal flow and the finite element method was used for the analysis. The authors established the critical flow velocity of molten metal down the sprue as 2.755 x 10^{3}mm/s. The results obtained were compared with the Reynolds number and literature. Various casts were produced and it was observed that sprue height below the critical drop height prevented casting defects.*

Keywords - *Critical Velocity, Finite Element Method, Continuity Equation, Mould Sprue*

I. INTRODUCTION

Casting a manufacturing process for making complex shapes of metal materials in mass production comprises of two main consecutive stages: filling process and solidification process. In filling process, the gating system comprising of the pouring cup, runner, sprue, sprue well and ingate, is designed to guide liquid metal into the mould cavity for filling. The riser system is used to compensate for shrinkage caused by casting solidification [3].

The main objective of a gating system is to lead clean molten metal poured from the ladle to the casting mould cavity, ensuring smooth, uniform and complete filling. Clean implies preventing the entry of slag and inclusions into the mould cavity, and minimizing surface turbulence. Smooth filling implies minimizing bulk turbulence. Uniform filling implies that all portions of the casting fill in a controlled manner, usually at the same time. Complete filling implies leading molten metal to thin and end sections with minimum resistance [9].

"Reference [3] optimised the design of gating/riser system in casting based on CAD and simulation technology. In it, one engine block was used to verify the effectiveness of the optimization method. Compared with the initial design, it was found that the optimized casting design can decrease porosity around 18% while the yield increases 16%."

"Reference [17] proposed a Taghuchi method based optimization technique for design of gating system using Magma Soft. Considering the multiple performance characteristics like filling velocity, shrinkage porosity and product yield, four gating parameters ingate height and width and runner height and width were optimized. ANOVA was used to analyze the effect of gating designs on cavity filling and casting quality and found that runner height and width are the most significant factors contributing more than 80%."

"Reference [1] investigated the formation of various casting defects and observed that various casting defects can be directly related to fluid flow phenomena involved in the stage of mould filling. They noted that, vigorous streams could cause mould erosion; highly turbulent flows could result in air and inclusions entrapments; and relatively slower filling might generate cold shuts." "Reference [6] in their work discovered that porosity a common casting defect resulted from improper design of gating system."

"Reference [2] noted that casting process engineers performed gating system design base on their individual knowledge and experience. In many cases, the gating system design is not optimal and often based on trial and error practice." "Reference [2] also noted that there are several casting design guidelines and empirical equations for the gating ratio, pouring time, and gating system dimensions, and that these variations in casting design guidelines and empirical equation chosen by different researchers have led to significant variations in casting design guidelines. These developments have forced foundries to carry out a number of trial and error runs and create guidelines based on their own experience."

"Reference [8] from his investigation concluded that aluminium castings are vulnerable to certain defects such as porosity, oxide inclusions, which are attributed to faulty design of gating system, turbulence during the moulding filling process with incorrect mould filling."

These problems not only lead to a long casting development cycle, but also a low reliability of casting design due to variations of individual knowledge and experience. Getting the liquid metal out of the crucible and into the mould is a critical step when making a casting: most casting scrap arises during this few seconds of pouring of the casting. Therefore, the authors seek to streamline the several casting design guidelines by establishing the critical velocity of molten metal flow in sand casting, gravity mould filling only having a top riser opened to atmospheric pressure using aluminium as the molten metal.

II. MATHEMATICAL MODEL OF MOLTEN METAL FLOW

"The proposed model for the numerical simulation of molten metal flow in the mould sprue is based on solving the conversation of mass equation (the continuity equations) in cylindrical axisymmetry coordinate [15]."

$$\frac{\partial P}{\partial t}+\frac{1}{r}\frac{\partial}{\partial r}(ru_r)+\frac{\partial u_z}{\partial z}=0 \qquad (1)$$

At steady state equation (1) becomes

$$\frac{1}{r}\frac{\partial}{\partial r}(ru_r)+\frac{\partial u_z}{\partial z}=0 \qquad (2)$$

The solutions to equation (2) can only be obtained by applying the appropriate initial and boundary conditions. Reference [7] gave the initial conditions for pressure and temperature fields as equation (3).

$$p(z,t_0)=p_0(z),\ T(r,z,t_0)=T_0(r,z) \qquad (3)$$

Reference [13] gave the boundary conditions specified in the considered problem as equations (4) to (7). Reference [5] applied these boundary conditions in their work "A unified analysis of filling and solidification in casting with natural convection"

At the inlet gate:

$$u_n=u_{in},u_t=0 \text{ or } p=p_{in} \qquad (4)$$

At the mould wall:

$$u_r=u_z=0,\quad \frac{\partial p}{\partial n}=0 \qquad (5)$$

At the flow front:

$$p=0 \qquad (6)$$

At the cavity centre line:

$$\frac{\partial p}{\partial n}=0,\ \frac{\partial u_t}{\partial r}=0,\ u_r=0,\ u_z=u \qquad (7)$$

This problem was solved using the finite element method in the weighted residuals formulation.

III. FINITE ELEMENT SOLUTION

The velocity distribution over the domain of interest is discretized into finite elements having *M* nodes, using suitable interpolation models for $u^{(e)}$ in element *e* as:

$$u_{(r,z)}=\sum_{i=1}^{m}w(r,z)u=[w]\{u\} \qquad (8)$$

and we developed the velocity distribution for equation (2) using the finite element method seeking an approximate solution over each finite element. The weighted residual and the weighted integral of equation (2) are equations (9) and (10) respectively.

$$w_{(r,z)}\left[\frac{1}{r}\frac{\partial u_r}{\partial r}+\frac{\partial u_z}{\partial z}\right]=0 \qquad (9)$$

$$\int_{\Omega_e}w_{(r,z)}\left[\frac{1}{r}\frac{\partial u_r}{\partial r}+\frac{\partial u_z}{\partial z}\right]drdz=0 \qquad (10)$$

We integrated equation (10) by parts (equation (11)), to obtain the weak form of equations (2)

$$-\int_{\Omega_e}\left(u_r\frac{1}{r}\frac{\partial w}{\partial r}+u_z\frac{\partial w}{\partial z}\right)\partial r\partial z+w\left(u_z+u_r\frac{1}{r}\right)\Big|_{\Omega_e}=0 \qquad (11)$$

The finite element model (equation (13)) was developed by substituting equations (8) and (10) into equation (11)

$$\int_{\Omega_e}w\left(\frac{1}{r}\frac{\partial w}{\partial r}+\frac{\partial w}{\partial z}\right)\partial r\partial z\{u\}=w\left(u_z+u_r\frac{1}{r}\right)\Big|_{\Omega_e} \qquad (12)$$

In matrix form equation (12) becomes

$$\left|K_{ij}{}^{e}\right|\{u\}=\left\{Q_{ij}{}^{e}\right\} \qquad (13)$$

Where $\left|K_{ij}{}^{e}\right|$ the M x M matrix is

$$\left|K_{ij}{}^{e}\right|=\int_{\Omega_e}w\left(\frac{1}{r}\frac{\partial w}{\partial r}+\frac{\partial w}{\partial z}\right)\partial r\partial z \qquad (14)$$

and $\left\{Q_{ij}^{e}\right\}$ represented by M x 1 column matrix is

$$\left\{Q_{ij}{}^{e}\right\}=w\left(u_z+u_r\frac{1}{r}\right)\Big|_{\Omega_e} \qquad (15)$$

To simplify the $\left|K_{ij}{}^{e}\right|$ and $\left\{Q_{ij}{}^{e}\right\}$, we used a linear rectangular element Fig. 1 to develop our interpolation model

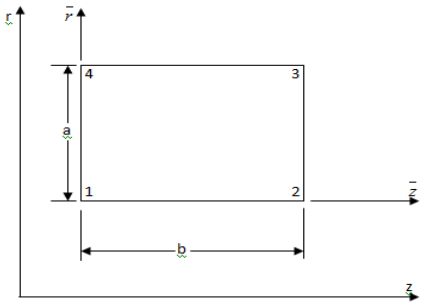

Fig. 1: Geometry of the element

Firstly, we obtained the interpolation model for the K^e matrices by considering an approximation of the form:

$$w(r,z)=c_1+c_2r+c_3z+c_4rz \qquad (16)$$

and used a linear rectangular element sides *a* and *b* (with *r* = *a* and *b* = *z*) (Fig. 1)

$w(r,z) = c_1 + c_2 a + c_3 b + c_4 ab$ (17) and require

$w_1 = w(0,0) = c_1;$ $w_2 = w(a,0) = c_1 + c_2 a;$

$w_3 = w(a,b) = c_1 + c_2 a + c_3 b + c_4 ab$

$w_4 = w(0,b) = c_1 + c_3 b$ (18) The solutions for $c_i (i = 1,...,4)$, in equations (18) are $c_1 = w_1;$

$$c_2 = \frac{w_2 - w_1}{a}; \quad c_3 = \frac{w_4 - w_1}{b};$$

$$c_4 = \frac{w_3 - w_4 + w_1 - w_2}{ab} \quad (19)$$

We substituted equations (19) into equation (17) and noting that a = r and b =z

$$w(r,z) = \left(1 - \frac{r}{a}\right)\left(1 - \frac{z}{b}\right)w_1 + \frac{r}{a}\left(1 - \frac{z}{b}\right)w_2 + \frac{rz}{ab}w_3 + \frac{z}{b}\left(1 - \frac{r}{a}\right)w_4 \quad (20)$$

$$w(r,z) = \theta_1 w_1 + \theta_2 w_2 + \theta_3 w_3 + \theta_4 w_4 \quad (21)$$

Where $\theta_1 = \left(1 - \frac{r}{a}\right)\left(1 - \frac{z}{b}\right);$ $\theta_3 = \frac{rz}{ab};$

$$\theta_2 = \frac{r}{a}\left(1 - \frac{z}{b}\right); \quad \theta_4 = \frac{z}{b}\left(1 - \frac{r}{a}\right) \quad (22)$$

We differentiated equations (22) with respect to *r* and *z* and obtained equations (23)

$$\frac{d\theta_1}{dr} = \left(-\frac{1}{a}\right)\left(1 - \frac{z}{b}\right) = \left(\frac{-1}{a} + \frac{z}{ab}\right)$$

$$\frac{d\theta_1}{dz} = \left(-\frac{1}{b}\right)\left(1 - \frac{r}{a}\right) = \left(\frac{-1}{b} + \frac{r}{ab}\right)$$

$$\frac{d\theta_2}{dr} = \frac{1}{a}\left(1 - \frac{z}{b}\right) = \frac{1}{a} - \frac{z}{ab}; \quad \frac{d\theta_2}{dz} = -\frac{r}{ab} \quad \frac{d\theta_3}{dr} = \frac{z}{ab};$$

$$\frac{d\theta_3}{dz} = \frac{r}{ab}; \quad \frac{d\theta_4}{dr} = -\frac{z}{ab};$$

$$\frac{d\theta_4}{dz} = \frac{1}{b}\left(1 - \frac{r}{a}\right) = \frac{1}{b} - \frac{r}{ab} \quad (23)$$

To derive the respective $|K_{ij}^{e}|$ we used a four linear rectangular element (Fig. 2) to obtain equations (24)

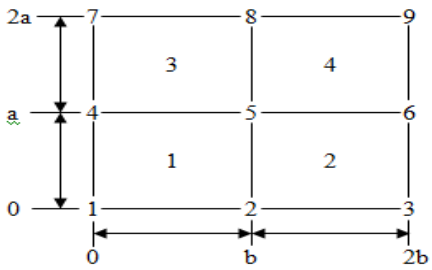

Fig. 2: Four Linear Rectangular Elements

$$K_{11}^{1} = \int_0^b \int_0^a \left[\left(\left(-\frac{1}{a}\right)\left(1 - \frac{z}{b}\right)\right)^2 + \left(\left(-\frac{1}{b}\right)\left(1 - \frac{r}{a}\right)\right)^2 \right] drdz$$

$$= \frac{a}{3b} + \frac{b}{3a}$$

$$K_{12}^{1} = \int_0^b \int_0^a \left[\left(\frac{-1}{a} + \frac{z}{ab}\right)^2 + \left(\frac{-1}{b} + \frac{r}{ab}\right)\left(-\frac{r}{ab}\right) \right] drdz$$

$$= \frac{a}{6b} + \frac{b}{3a}$$

$$K_{13}^{1} = \int_0^b \int_0^a \left[\left(\frac{-1}{a} + \frac{z}{ab}\right)\left(\frac{z}{ab}\right) + \left(\frac{-1}{b} + \frac{r}{ab}\right)\left(\frac{r}{ab}\right) \right] drdz$$

$$= \frac{-a}{6b} - \frac{b}{6a}$$

$$K_{14}^{1} = \int_0^b \int_0^a \left[\left(\frac{-1}{a} + \frac{z}{ab}\right)\left(\frac{-z}{ab}\right) + \left(\frac{-1}{b} + \frac{r}{ab}\right)\left(\frac{1}{b} - \frac{r}{ab}\right) \right] drdz$$

$$= \frac{a}{3b} + \frac{b}{6a}$$

$$K_{21}^{1} = K_{12}^{1} = \frac{a}{6b} + \frac{b}{3a}$$

$$K_{22}^{1} = \int_0^b \int_0^a \left[\left(\frac{1}{a} - \frac{z}{ab}\right)^2 + \left(-\frac{r}{ab}\right)^2 \right] drdz$$

$$= \frac{a}{3b} + \frac{b}{3a}$$

$$K_{23}^{1} = \int_0^b \int_0^a \left[\left(\frac{1}{a} - \frac{z}{ab}\right)\left(\frac{z}{ab}\right) + \left(\frac{-r}{ab}\right)\left(\frac{r}{ab}\right) \right] drdz$$

$$= \frac{b}{6a} - \frac{a}{3b}$$

$$K_{24}^{1} = \int_0^b \int_0^a \left[\left(\frac{1}{a} - \frac{z}{ab}\right)\left(\frac{-z}{ab}\right) + \left(\frac{-r}{ab}\right)\left(\frac{1}{b} - \frac{r}{ab}\right) \right] drdz$$

$$= \frac{b}{6a} - \frac{a}{6b}$$

$$K_{31}^{1} = K_{13}^{1} = \frac{-a}{6b} - \frac{b}{6a}$$

$$K_{32}^{1} = K_{23}^{1} = \frac{b}{6a} - \frac{a}{3b}$$

$$K_{33}^1 = \int_0^b \int_0^a \begin{bmatrix} \left(\frac{z}{ab}\right)^2 + \\ \left(\frac{r}{ab}\right)^2 \end{bmatrix} drdz = \frac{a}{3b} + \frac{b}{3a}$$

$$K_{34}^1 = \int_0^b \int_0^a \begin{bmatrix} \left(\frac{z}{ab}\right)\left(\frac{-z}{ab}\right) \\ + \left(\frac{r}{ab}\right)\left(\frac{1}{b} - \frac{r}{ab}\right) \end{bmatrix} drdz$$

$$= \frac{a}{6b} - \frac{b}{3a}$$

$$K_{41}^1 = K_{14}^1 = \frac{a}{3b} + \frac{b}{6a}$$

$$K_{42}^1 = K_{24}^1 = \frac{b}{6a} - \frac{a}{6b}$$

$$K_{43}^1 = K_{34}^1 = \frac{a}{6b} - \frac{b}{3a}$$

$$K_{44}^1 = \int_0^b \int_0^a \left[\left(\frac{-z}{ab}\right)^2 + \left(\frac{1}{b} - \frac{r}{ab}\right)^2\right] drdz$$

$$= \frac{a}{3b} + \frac{b}{3a}$$

(24)

The $\left|K_{ij}^e\right|$ matrix is therefore equation (25)

$$K = \begin{bmatrix} \frac{a}{3b}+\frac{b}{3a} & \frac{a}{6b}+\frac{b}{3a} & \frac{-a}{6b}-\frac{b}{6a} & \frac{a}{3b}+\frac{b}{6a} \\ \frac{a}{6b}+\frac{b}{3a} & \frac{a}{3b}+\frac{b}{3a} & \frac{b}{6a}-\frac{a}{3b} & \frac{b}{6a}-\frac{a}{6b} \\ \frac{-a}{6b}-\frac{b}{6a} & \frac{b}{6a}-\frac{a}{3b} & \frac{a}{3b}+\frac{b}{3a} & \frac{a}{6b}-\frac{b}{3a} \\ \frac{a}{3b}+\frac{b}{6a} & \frac{b}{6a}-\frac{a}{6b} & \frac{a}{6b}-\frac{b}{3a} & \frac{a}{3b}+\frac{b}{3a} \end{bmatrix}$$

$$K = \frac{b}{6a}\begin{bmatrix} 2 & -2 & -1 & 1 \\ -2 & 2 & 1 & -1 \\ -1 & - & 2 & -2 \\ 1 & -1 & -2 & 2 \end{bmatrix} +$$

$$\frac{a}{6b}\begin{bmatrix} 2 & 1 & -1 & -2 \\ 1 & 2 & -2 & -1 \\ -1 & -2 & 2 & 1 \\ -2 & -1 & 1 & 2 \end{bmatrix} \qquad (26)$$

If $a = 4$ and $b = 1$ equation (26) becomes

$$K = \begin{bmatrix} 1.4166 & 0.5834 & -0.7084 & -1.2916 \\ 0.5834 & 1.4166 & -1.2916 & -0.7084 \\ -0.7084 & -1.2916 & 1.4166 & 0.5834 \\ -1.2916 & -0.7084 & 0.5834 & 1.4166 \end{bmatrix} \qquad (27)$$

Let, $K^1 = K^2 = K^3 = K^4$, therefore

$$K^e = K^1 + K^2 + K^3 + K^4 \qquad (28)$$

$$K_{ij}^e = \begin{bmatrix} \begin{bmatrix} 1.4166 & 0.5834 & -0.7084 & -1.2916 \\ 0.5834 & 1.4166 & -1.2916 & -0.7084 \\ -0.7084 & -1.2916 & 1.4166 & 0.5834 \\ -1.2916 & -0.7084 & 0.5834 & 1.4166 \end{bmatrix} + \\ \begin{bmatrix} 1.4166 & 0.5834 & -0.7084 & -1.2916 \\ 0.5834 & 1.4166 & -1.2916 & -0.7084 \\ -0.7084 & -1.2916 & 1.4166 & 0.5834 \\ -1.2916 & -0.7084 & 0.5834 & 1.4166 \end{bmatrix} + \\ \begin{bmatrix} 1.4166 & 0.5834 & -0.7084 & -1.2916 \\ 0.5834 & 1.4166 & -1.2916 & -0.7084 \\ -0.7084 & -1.2916 & 1.4166 & 0.5834 \\ -1.2916 & -0.7084 & 0.5834 & 1.4166 \end{bmatrix} + \\ \begin{bmatrix} 1.4166 & 0.5834 & -0.7084 & -1.2916 \\ 0.5834 & 1.4166 & -1.2916 & -0.7084 \\ -0.7084 & -1.2916 & 1.4166 & 0.5834 \\ -1.2916 & -0.7084 & 0.5834 & 1.4166 \end{bmatrix} \end{bmatrix} \qquad (29)$$

The assembled K_{ij}^e matrix using Fig. 2 is equation (30) and (31)

We applied the boundary conditions (equations (4) to (7)) to equation (15), and obtained equation (32)

$$\{Q_{ij}^e\} = \begin{Bmatrix} 0 \\ 0 \\ 0 \\ 0 \\ 1 \\ 0 \\ 0 \\ 1 \\ 0 \end{Bmatrix} \qquad (32)$$

We substituted equation (31) and (32) into equation (13) and obtained (33)

IV. Results and Discussion

Table I shows the results for the finite element analysis. Fig. 3, are the graphs of velocity against nodal values showing the velocity profile at different cross sections along the mould's sprue. These profiles are parabolic in shape with the maximum velocity at the centre.

TABLE I: RESULTS OF FINITE ELEMENT ANALYSIS FOR Z = *1MM*

Nodes	u	Velocity (mm/s)
1	u_1	1.1352
2	u_2	1.1308
3	u_3	0.0000
4	u_4	1.0288
5	u_5	1.3255
6	u_6	0.0000
7	u_7	0.7537
8	u_8	1.7230
9	u_9	0.0000

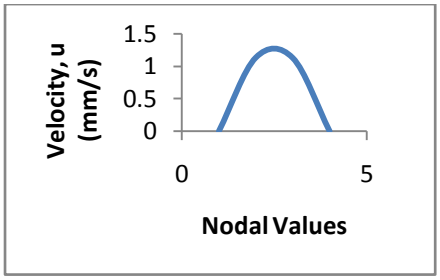

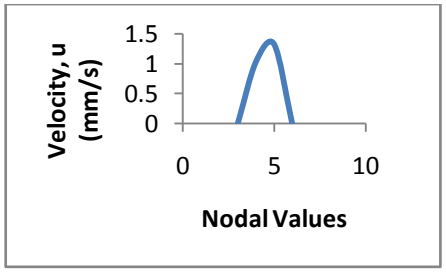

Figs. 3: Graphs of velocity against nodal values showing the velocity profile at different cross sections along the mould's sprue

$$K_{ij}^{\ e}=\begin{bmatrix} K_{11}^1 & K_{12}^1 & 0 & K_{14}^1 & K_{13}^1 & 0 & 0 & 0 & 0 \\ K_{21}^1 & K_{22}^1+K_{11}^2 & K_{12}^2 & K_{24}^1 & K_{23}^1+K_{14}^2 & K_{23}^2 & 0 & 0 & 0 \\ 0 & K_{21}^2 & K_{22}^2 & 0 & K_{24}^2 & K_{23}^2 & 0 & 0 & 0 \\ K_{41}^1 & K_{42}^2 & 0 & K_{44}^1+K_{11}^3 & K_{43}^1+K_{12}^3 & 0 & K_{14}^3 & K_{13}^3 & 0 \\ K_{31}^1 & K_{32}^1+K_{41}^2 & K_{42}^2 & K_{34}^1+K_{21}^3 & K_{33}^1+K_{44}^2+K_{22}^3+K_{11}^4 & K_{43}^2+K_{12}^4 & K_{24}^3 & K_{23}^3+K_{14}^4 & K_{13}^4 \\ 0 & K_{31}^2 & K_{32}^2 & 0 & K_{34}^2+K_{21}^4 & K_{33}^2+K_{22}^4 & 0 & K_{24}^4 & K_{23}^4 \\ 0 & 0 & 0 & K_{41}^3 & K_{42}^4 & 0 & K_{44}^4 & K_{43}^4 & 0 \\ 0 & 0 & 0 & K_{31}^3 & K_{32}^3+K_{41}^4 & K_{42}^4 & K_{34}^3 & K_{33}^3+K_{44}^4 & K_{43}^4 \\ 0 & 0 & 0 & 0 & K_{31}^4 & K_{32}^4 & 0 & K_{34}^4 & K_{33}^4 \end{bmatrix} \quad (30)$$

$$K_{ij}^{\ e}=\begin{bmatrix} 1.4166 & 0.5834 & 0 & -1.2916 & -0.7084 & 0 & 0 & 0 & 0 \\ 0.5834 & 2.8332 & 0.5834 & -0.7084 & -2.5832 & -1.2916 & 0 & 0 & 0 \\ 0 & 0.5834 & 1.4166 & 0 & -0.7084 & -1.2916 & 0 & 0 & 0 \\ -1.2916 & -0.7084 & 0 & 2.8331 & 1.1668 & 0 & -1.2916 & -0.7084 & 0 \\ -0.7084 & -2.5832 & -0.7084 & 2 & 5.6664 & 1.1668 & -0.7084 & -2.5832 & -0.7084 \\ 0 & -0.7084 & -1.2916 & 0 & 1.1668 & 1.1668 & 0 & -0.7084 & -1.2916 \\ 0 & 0 & 0 & -0.7084 & -1.2916 & 0 & 0.5834 & 1.4166 & 0 \\ 0 & 0 & 0 & -0.7084 & -2.5832 & -0.7084 & 0.5834 & 2.8332 & 0.5834 \\ 0 & 0 & 0 & 0 & -0.7084 & -1.2916 & 0 & 0.5834 & 1.4166 \end{bmatrix} \quad (31)$$

$$\begin{bmatrix} 1.4166 & 0.5834 & 0 & -1.2916 & -0.7084 & 0 & 0 & 0 & 0 \\ 0.5834 & 2.8332 & 0.5834 & -0.7084 & -2.5832 & -1.2916 & 0 & 0 & 0 \\ 0 & 0.5834 & 1.4166 & 0 & -0.7084 & -1.2916 & 0 & 0 & 0 \\ -1.2916 & -0.7084 & 0 & 2.8331 & 1.1668 & 0 & -1.2916 & -0.7084 & 0 \\ -0.7084 & -2.5832 & -0.7084 & 2 & 5.6664 & 1.1668 & -0.7084 & -2.5832 & -0.7084 \\ 0 & -0.7084 & -1.2916 & 0 & 1.1668 & 1.1668 & 0 & -0.7084 & -1.2916 \\ 0 & 0 & 0 & -0.7084 & -1.2916 & 0 & 0.5834 & 1.4166 & 0 \\ 0 & 0 & 0 & -0.7084 & -2.5832 & -0.7084 & 0.5834 & 2.8332 & 0.5834 \\ 0 & 0 & 0 & 0 & -0.7084 & -1.2916 & 0 & 0.5834 & 1.4166 \end{bmatrix} \begin{Bmatrix} u_1 \\ u_2 \\ u_3 \\ u_4 \\ u_5 \\ u_6 \\ u_7 \\ u_8 \\ u_9 \end{Bmatrix} = \begin{Bmatrix} 0 \\ 0 \\ 0 \\ 0 \\ 1 \\ 0 \\ 0 \\ 1 \\ 0 \end{Bmatrix} \quad (33)$$

The results obtained were compared with the Reynolds Number (Re)

$$Re=\frac{\rho V h}{\mu}=\frac{2.8\times10^{-6}\times2754.81\times386.80}{0.00296}=1007.96$$

(32) where V is the velocity of the liquid, ρ is the density of the liquid, h is a characteristic linear dimension of the geometry of the flow path, and μ is the viscosity.

Values of Reynolds number below the critical Reynolds number (2000) will prevent air entrainment and porosity problem in casting, because flow is smooth and laminar. The Reynolds number obtained from this work (*1,007.96*) is below the critical Reynolds number (*2,000*), therefore, the critical velocity (*2755mm/s*) and critical drop height (*387mm*) obtained in this work will prevent casting defects associated with pouring velocities above the critical velocity because flow is smooth and laminar.

The maximum velocity of molten metal flow obtained from this work (**2755mm/s**), when compared with the work of Rohaya [13] (Table II and Fig. 4) (which ranged from 2300mm/s to 3200mm/s) showed that the danger of casting defects as a result of molten metal flow above the critical velocity can be avoided.

TABLE II: COMPARISON BETWEEN THIS WORK AND ROHAYA, [13]

Z	This Work	Rohaya
1	130.76	500
2	2135.54	2300
3	2754.81	3200
4	0.00	0.00

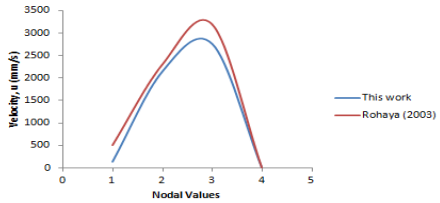

Figure 4: Graph of velocity against nodal values showing the velocity profile at a cross section along the sprue for this work and Rohaya, [13]

The solutions obtained from this work (**2755mm/s**) were also compared with the work of Feng [3] (Table III and Fig. 5) (which ranged from 260mm/s to 2850mm/s), the comparison showed that the danger of air entrainment leading to defect as a result of molten metal flow above the critical velocity can be avoided.

TABLE III: COMPARISON BETWEEN THIS WORK AND FENG [3]

Z	This Work	Feng
1	130.76	260
2	2135.54	2450
3	2754.81	2850
4	0	0

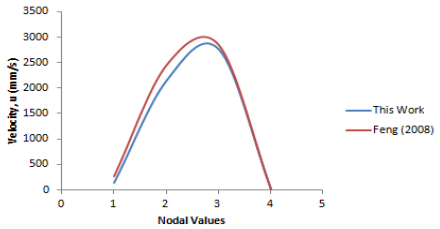

Fig. 5: Graph of velocity against nodal values showing the velocity profile at a cross section along the sprue for this work and Feng [3]

To validate the results from this work, we used the results obtained to produce various cast. The cast produced showed that sprue height below the critical drop height prevented casting defects associated with pouring velocities above the critical velocity while sprue height above the critical drop height the danger of casting defects associated with pouring velocities above the critical velocity could not be avoided.

Fig. 6, showed the various casting defects that can occur when cast are produced using sprue height above the critical drop height (387mm): The melt is not safe from the various casting defects because the pouring velocity exceeded the critical velocity. These defects can be avoided with pouring velocities below the critical velocity (Fig.7).

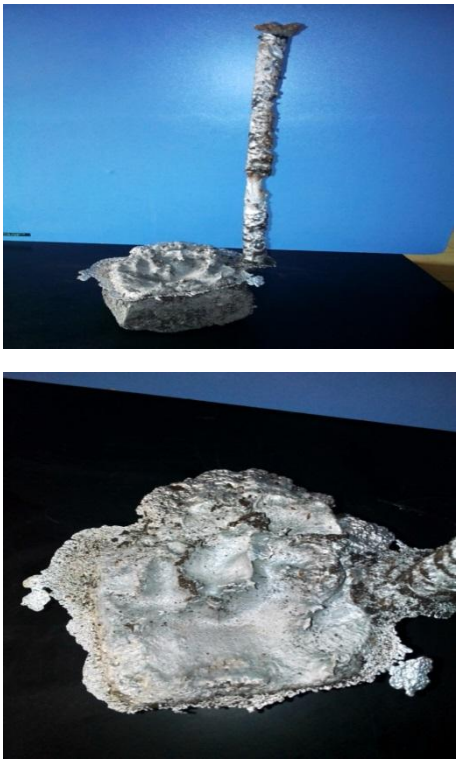

Fig. 6: Casts produced for sprue height above the critical drop height

Fig 7: Cast produced using sprue height below the critical drop height

It is evident from Fig. 7 that all casting defects associated with pouring using sprue height above the critical drop height can be avoided if cast can be produced using sprue heights below the critical drop height. In this case the melt is safe since the pouring velocity is below the critical velocity.

V. Conclusion

The authors used the finite element method to obtain the critical flow velocity of molten metal in the mould sprue and the critical drop height. The weighted integral of the continuity equation was obtained, the weak form of the equation was developed and the finite element model was determined. The various matrices were assembled, solved and solutions

obtained by using a four linear rectangular element. Using appropriate interpolation function and boundary conditions, the solutions to the equations were obtained. Comparing solutions with relevant literatures and the Reynolds Number showed that molten metal flow below the critical velocity would prevent casting defects because flow is smooth and laminar.

The critical drop height obtained from this work was used to produce various casts. The results obtained showed that casting defects can be avoided when cast are produced using sprue height below the critical drop height while cast produced using sprue height above the critical drop height the danger of casting defects could not be avoided. Consequently, foundry engineers will no longer rely on their individual knowledge and experience or perform a number of trial and error runs before carrying out any casting process. This will reduce casting development cycle, defects and production time.

REFERENCES

[1] E. H. Attar, R.P. Babaei, K. Asgari, P. Davami, "Modelling of air pressure effects in casting moulds". Journal of Modelling and Simulation in Materials Science and Engineering 13, pp. 903-917, 2005.

[2] J. Campbell, Materials Solutions Conference on Aluminium Casting Technology,Chicago, 3. 1998

[3] L. Feng, "Optimized Design of Gating/Riser System in Casting Based on CAD and Simulation Technology". Submitted to the faculty of the Worchester Polytechnic Institute in partial fulfillment of the requirements for degree of Master of Science in Manufacturing Engineering, (2008)

[4] V. D. Hutton, "Fundaments of Finite Element Analysis", 1st Edition, McGraw-Hill Companies, Inc. (2004) pp 293 - 295

[5] I. Ik-Tae, K. Woo-Seung, L. Kwan-Soo, "A unified analysis of filling and solidification in casting with natural convection" International Journal of Heat and Mass Transfer, 44, pp. 1507 – 1515, 2001

[6] P. D. Lee, A. Chirazi, D. See, "Modelling micro porosity in Aluminium - Silicon alloys: a review". Journal of Light Metals, vol. 1, pp. 15-30, 2001.

[7] B. Mochacki, J. S. Suchy, "Numerical Methods in Computations of Foundry Processes". Polish Foundrymen's Technical Association Publishers, Krakow (1995).

[8] B. Ravi. "Computer-aided Casting Design and Simulation". Short Term Training Program V.N.I.T. Nagpur, July 21, (2009)

[9] B. Ravi, "Metal Casting". Computer-Aided Design and Analysis, 4th Edition, Prentice-Hall, New Delhi, India (2005).

[10] J. N. Reddy, "An Introduction to the Finite Element Method". Third Edition, International Edition McGraw-Hill Inc. pp. 146 – 147, 441 – 442, 2006.

[11] B. D. Rohaya,"Design and Analysis of Casted LM6 - TIC in Designing of Production Tooling",Faculty of Manufacturing Engineering, Universiti Teknikal Malaysia Melaka (UTEM) pp. 63 – 69, 2013

[12] S. R. Singiresu, "The Finite Element Methods in Engineering", fourth edition, Elsevier Science and Technology Books Publisher (2004).

[13] L. Sowa, "Model of the Casting Solidification taking into consideration the motion of liquid phase". Archives of Mechanical technology and Automatization, vol 18, pp.287 – 296, 1998

[14] L. Sowa, "Numerical Analysis of the Thermal and Fluid Flow Phenomena of the Fluidity test". Archives of Foundry Engineering, Volume 10 Issue 1, pp. 157 – 160, 2010.

[15] L. Sowa, A. Bokota, "Numerical Modelling of Thermal and Fluid Flow Phenomena in the Mould Channel". Archives of Foundry, vol. 7, Issue 4, pp. 165 – 168, 2007.

[16] L. Sowa, N. Sczygiol, T. Domoilski, A, Bokota, "Simplified Model of Metal Solidification in the Thin Plane Cavity of the Casting Mould". Archives of Foundry Engineering, Volume 8 special Issue 1, pp. 309 – 312, 2008

[17] Zhizhong S., Hu H., Chen X., "Numerical Simulation of Gating System parameters of a Magnesium Alloy Casting with Multiple Performance Characteristics". Journal of Material. Processing Tech., Vol.199, pp.256-264, 2008.